hexagon:2611.00595v1

Prime Knots with Augmentation-Rank Gaps at Unbounded Bridge Number

Roy van Rijn

Abstract

We construct explicit braid families containing infinitely many distinct hyperbolic prime knots of each bridge number $b = 5, 6$ and each sufficiently large b, with complex augmentation rank at most $b - 1$ and meridional rank b. Alternating-group colorings force b meridional generators, while two fixed meridian words let a local rank-one obstruction persist as the braid grows. An oriented diagram isotopy realizes the associated two-cusped exteriors as fillings of a single three-cusped exterior. Rigorous interval certificates establish hyperbolicity of that exterior and the two small-bridge exteriors used in the filling argument.

1 Introduction

How far can one get in determining the bridge number of a knot using rank-one meridian representations? For a knot $K \subset S^3$, the meridional rank $\mathrm{mr}(K)$ is the least number of positive meridians generating its group, and the bridge number $\mathrm{br}(K)$ is the least number of maxima in a bridge presentation. The conventional complex augmentation rank $\mathrm{ar}_{\mathbb{C}}(K)$ uses the cord algebra with $U = 1$ and meridian parameter different from 1. By Cornwell's correspondence it is the maximum dimension of an irreducible complex representation in which a meridian is diagonalizable with eigenvalues $1, \ldots, 1, \mu$, where $\mu \neq 0, 1$ [1, Theorem 1.2 and Definition 1.8]. Meridians are conjugate, so this condition holds for every meridian. The inequalities

$$\mathrm{ar}_{\mathbb{C}}(K) \leq \mathrm{mr}(K) \leq \mathrm{br}(K)$$

give two ways to bound bridge number from below. We construct prime knots of arbitrarily large bridge number for which the first bound falls short and the second is an equality.

Read braid words from left to right, from top to bottom, and write σ_i for the positive crossing at positions $i, i+1$. Let

$$U = \sigma_1\sigma_2\sigma_3^{-2}\sigma_2\sigma_3^{-2}\sigma_2\sigma_1^2\sigma_2^3\sigma_3^{-1} \in B_4.$$

For $b \geq 5$, put $d = b - 2$ and embed U in B_b on the first four strands. Define

$$\delta_b = \sigma_2(\sigma_3\sigma_4\sigma_3^{-1})\sigma_5 \cdots \sigma_{b-1}, \qquad K_{b,k} = U\delta_b^{\widehat{(d+1)(1+d^2k)}} \quad (k \geq 0).$$

An empty product is the identity.

Theorem 1. *For every integer $b \geq 5$ and $k \geq 0$, $K_{b,k}$ is a knot and*

$$\mathrm{ar}_{\mathbb{C}}(K_{b,k}) \leq b - 1 < \mathrm{mr}(K_{b,k}) = \mathrm{br}(K_{b,k}) = b.$$

For each $b = 5, 6$ and each sufficiently large b, all sufficiently large k give hyperbolic prime knots, and infinitely many distinct knot types occur for that fixed b.

Cornwell proved $2 = \mathrm{ar}_{\mathbb{C}}(K) < \mathrm{mr}(K) = 3$ for the four knots $8_{16}, 8_{17}, 10_{91}, 10_{94}$ and their mirrors. His rank-gap classification assumes crossing number at most ten and bridge number and braid index both equal to three, and its augmentation upper bounds use Gröbner bases of braid-specific equations [1, Corollary 1.12 and Theorem 5.3]. Theorem 1 gives infinite hyperbolic prime families at unbounded bridge number. Gao, Gu, Li and Wang prove $\mathrm{ar}_{\mathbb{C}} \leq 5 < \mathrm{mr} = \mathrm{br} = 6$ for the untwisted Whitehead double of the square knot, using its satellite presentation for the augmentation bound and a finite quotient and cocycle calculation for the meridional bound [3, Theorem 1.3 and Section 6]. Here the rank-one obstruction persists under a family of braid tails, and the diagram isotopy produces hyperbolic examples without taking satellites or connected sums. The theorem gives an upper bound on augmentation rank. Its hyperbolicity cutoffs are existential, and the cutoff in k is allowed to depend on b.

The algebraic construction uses the same braid action in two ways. The braid after U fixes the first and fourth meridians. After conjugating the labels on strands five through b by the fourth label, this part of the braid acts by ordinary Hurwitz moves on the remaining entries. These moves preserve their ordered product. In an alternating group we can compute the order of this product explicitly and use it to close up a coloring that needs b generators. In a rank-one representation, assuming that both the displacement vectors and their covectors are independent forces two matrix identities inside U. Seven signed crossing relations then give a contradiction.

The two filling steps use different peripheral markings. The first filling uses the disk marking of a cusp of the fixed three-cusped exterior. The homeomorphism to the two-cusped parent is unmarked and transfers hyperbolicity. The second filling uses the original disk marking of the circle in that parent.

To obtain the two-cusped parent, put a circle around the strands carrying the Hurwitz moves. Varying k amounts to filling that circle. The number of strands through it varies with b, so a separate argument is needed to control the exteriors before filling. The diagram isotopy in Section 4 trades each extra threaded curl for a full twist between a knot arc and a circle arc. This identifies all the two-cusped exteriors with fillings of a single three-cusped manifold, to which we apply hyperbolic Dehn filling twice.

2 Alternating-group colorings

For any group, the Wirtinger rule at a positive braid crossing is $T(a, c) = (c, c^{-1}ac)$; its inverse is $T^{-1}(a, c) = (aca^{-1}, a)$. A tuple of labels at the top of a closed braid defines a homomorphism from the knot group exactly when the crossing rules return the tuple at the bottom. The image is generated by the top labels, because they generate the Wirtinger group.

Put $g = \sigma_3\sigma_4\sigma_3^{-1}$. On the entries (a, C, e) at positions $3, 4, 5$, its action is

$$(CeC^{-1},\ C,\ e^{-1}C^{-1}aCe).$$

In particular, g fixes the fourth label and acts as T on (a, CeC^{-1}). The subgroup of B_b generated by $\sigma_2, g, \sigma_5, \ldots, \sigma_{b-1}$ fixes entries one and four and acts by adjacent Hurwitz moves on the tuple

$$(M_2, M_3, CM_5C^{-1}, \ldots, CM_bC^{-1}), \qquad C = M_4. \tag{1}$$

This follows for the last generators because simultaneous conjugation commutes with T, and then holds for inverses as well. The product of the entries in (1) is invariant, since $T(a, c)$ has product ac.

We use permutations composed from right to left. The top labels on $2b$ symbols are

$$x_0 = (0\,1)(2\,3), \quad x_1 = (1\,4)(2\,3),$$
$$x_2 = (0\,5)(1\,6), \quad x_3 = (1\,2)(6\,7),$$
$$x_4 = (0\,8)(7\,9), \quad x_j = (2j-2\ 2j)(2j-1\ 2j+1) \quad (5 \le j < b).$$

The first four generate A_8. Indeed, x_0x_1 is a three-cycle on $\{0,1,4\}$. By conjugating that cycle by x_2 and x_3, then conjugating the resulting cycles by x_3 and x_0, respectively, we obtain the additional supports

$$\{4,5,6\}, \quad \{0,2,4\}, \quad \{4,5,7\}, \quad \{1,3,4\}.$$

These cycles generate A_8. To see the enlargement at each step, an alternating group on an old set of at least three symbols together with a three-cycle on two old symbols and one new symbol generates the alternating group on the union. Conjugations and inverses give both orientations for every pair of old symbols, including when the old set has size three. If the cycle has just one old symbol, conjugate it by an old permutation moving that symbol. The product of the original cycle with the inverse conjugate gives a cycle on two old symbols and one new symbol, after which the other new symbol can also be added. The displayed supports can therefore be adjoined in order. Each x_j for $j \ge 4$ consists of two transpositions $(a\,u)(c\,v)$ with distinct old symbols a, c and distinct new symbols u, v. Conjugate it by an even old permutation fixing c and moving a, and multiply the two double transpositions. This gives a three-cycle on two old symbols and u. Repeat with a, u fixed and c moved to adjoin v. The full tuple generates A_{2b}.

To check the coloring, let $X = x_1,\ Y = x_2,\ C = x_3$. Applying the crossing rule through U gives

$$(x_0, a, h, C, x_4, \ldots, x_{b-1}), \qquad a = (0\,5)(1\,4), \quad h = (1\,6)(2\,3).$$

This four-strand calculation can also be read from the crossing relations in (2). With $z_i = Cx_{i+3}C^{-1}$ for $1 \le i \le d-2$, the product of the middle tuple $(a, h, z_1, \ldots, z_{d-2})$ is

$$p = (0\,8\,10 \cdots 2b-2\ 5)(1\,6\,9\,11 \cdots 2b-1\ 4)(2\,3).$$

In each displayed progression the terms run only up to the indicated endpoint. For $b = 5$ the product is the one computed below. For larger b each additional factor inserts its two new symbols just before 5 and 4 in the respective cycles. The two long cycles have lengths d and $d+1$, so p has order $d(d+1)$. Reading the cycles gives

$$pXp^{-1} = h, \qquad p^iYp^{-i} = z_i\ (1 \le i \le d-2), \qquad p^dYp^{-d} = a.$$

The adjacent moves in δ_b act on (1) as the left shift that sends the first entry m to $p^{-1}mp$ at the end. After d shifts all labels have been conjugated by p^{-1}. After $d+1$ shifts the three displayed identities return the initial middle tuple $(X, Y, z_1, \ldots, z_{d-2})$. Adding $d^2(d+1)k$ shifts has no effect because p has order $d(d+1)$.

Example. At $b = 5$ the middle tuple has length three and $p = (0\,8\,5)(1\,6\,9\,4)(2\,3)$. Four shifts close the coloring of $U(\sigma_2 g)^4$, and a further 36 shifts act trivially. This gives the exponent $4 + 36k$ on five strands.

The strand permutation of δ_b is a d-cycle on positions $\{2, 3, 5, \ldots, b\}$; its exponent is 1 mod d. The permutation of U is $(1\,2)(3\,4)$. The two transpositions insert the two omitted positions into that cycle, giving one knot component. Its group surjects onto A_{2b} by the coloring just constructed. A double transposition moves two independent directions in the natural

permutation representation over $\mathbb{C}$. The following lower bound uses its two transposition edges. A set of at most $b-1$ double transpositions has a support graph with at most $2b-2$ edges on $2b$ vertices. Each generator preserves the components of the graph, so such a set cannot generate a transitive group. The quotient forces $\mathrm{mr}(K_{b,k}) \geq b$, since every positive meridian is conjugate to a top label. A closed b-strand braid gives a bridge presentation with at most b maxima, and the Wirtinger relations of a bridge presentation give one generating meridian per bridge. Thus $\mathrm{mr}(K_{b,k}) = \mathrm{br}(K_{b,k}) = b$.

3 The rank-one obstruction

We prove an upper bound for every knot obtained by following U with a braid in the subgroup acting on (1). That subgroup fixes the first and fourth meridian words. These two fixed positions suffice for the rank-one argument.

Lemma 2. *Suppose that τ belongs to $\langle \sigma_2, g, \sigma_5, \ldots, \sigma_{b-1} \rangle$ and $\widehat{U\tau}$ is a knot. Let its group act on a finite-dimensional space V over a field so that each meridian has displacement of rank one. Write each meridian as $M = I - uf$, where $u \in V$ and $f \in V^*$. Then at least one of the spans of all the u's and all the f's has dimension at most $b-1$, and both dimensions are at most b.*

Proof. Each of the two spans is already spanned by its b top-strand vectors or covectors. The root span of the generating meridians is invariant under those generators and their inverses, and the covector span is invariant under right multiplication by the same matrices. Conjugating a generator therefore introduces neither a new root direction nor a new covector direction.

Suppose both spans have dimension b. In particular both families of four vectors and covectors on the first four strands are separately independent. Set

$$\mu = \det M \neq 0, \qquad f(u) = 1 - \mu, \qquad M^{-1} = I + \mu^{-1} uf.$$

The first two identities hold for every meridian, with one common μ. When $M_a = I - u_a f_a$, conjugation by a matrix J replaces its pair by $(Ju_a, f_a J^{-1})$. Two pairs for the same nonzero displacement differ by reciprocal scaling.

Here is the crossing trace through U. We use arc subscripts on the matrices M_i in this proof. A row (o, a, c, ϵ) represents $M_c = M_o^{\epsilon} M_a M_o^{-\epsilon}$. The input labels are $(1, 0, 8, 13)$ and the output labels are $(1, 6, 16, 13)$.

0	0	1	2	$-$	1	8	2	3	$-$
2	3	13	14	$+$	3	14	3	4	$+$
4	4	8	9	$-$	5	9	14	15	$+$
6	15	9	10	$+$	7	10	4	5	$-$
8	10	0	1	$-$	9	1	10	11	$-$
10	5	11	12	$-$	11	12	5	6	$-$
12	6	12	13	$-$	13	13	15	16	$+$

(2)

The repeated outer labels express closure, since τ fixes the first and fourth entries. Each row is obtained by T or T^{-1} in the order of the letters in U.

Put $A = M_2,\ B = M_8,\ C = M_{13},\ D = M_0$. Replacing M_1 by $A = D^{-1} M_1 D$ changes the root by a multiple of the root of D and the covector by a multiple of its covector, preserving both independent families. Let H and F denote the root and covector spans of A, B, C, respectively.

Both have dimension three, and in the pair (v,ν) of D one has $v \notin H$ and $\nu \notin F$. Rows 1 through 7 and row 13 propagate pairs in H, F.

Rows 0 and 8 give $DAD^{-1} = X^{-1}DX$ for $X = M_{10}$. If A, X have pairs (a, f) and (x, ξ) in H, F, comparing the pairs on both sides gives

$$a - \nu(a)v = \lambda\big(v + \mu^{-1}\xi(v)x\big),$$
$$f + \mu^{-1}f(v)\nu = \lambda^{-1}\big(\nu - \nu(x)\xi\big)$$

for some $\lambda \neq 0$. The coefficients on v, ν give $\lambda = -\nu(a)$ and $f(v) = \mu\lambda^{-1}$. The other components give $a = \lambda\mu^{-1}\xi(v)x$ and $f = -\lambda^{-1}\nu(x)\xi$. Applying ν to the expression for a gives $\nu(x)\xi(v) = -\mu$. Thus $af = x\xi$ and $X = A$. The relation is now $DAD = ADA$. Row 9, together with $M_1 = DAD^{-1}$, gives $M_{11} = D$.

Next, rows 10–12 send (D, P) to (P, N), then (N, Q), then (Q, C), where $P = M_5$, $N = M_{12}$ and $Q = M_6$. Write the pair of P as (p, π) in H, F, and put $x_1 = \pi(v)$, $y_1 = \nu(p)$, $h_1 = 1 + x_1y_1/\mu$. Conjugating at each step gives

	root	covector
N	$v + (x_1/\mu)p$	$\nu - y_1\pi$
Q	$y_1v + h_1p$	$-(x_1/\mu)\nu + h_1\pi$
C	$h_1v + (x_1/\mu)(1+h_1)p$	$h_1\nu - y_1(1+h_1)\pi.$

For example $N = P^{-1}DP$; the next row uses $Q = N^{-1}PN$. The last pair lies in H, F, so $h_1 = 0$ and $x_1y_1 = -\mu$. Its remaining coefficients multiply to one, which gives $P = C$.

Of the eight rows supported in H, F, rows 1–7 suffice for the contradiction. They now satisfy the hypotheses of Lemma 3 and contain the three independent pairs of A, B, C. This proves the span bound. □

Lemma 3. *Suppose the rank-one meridian matrices of common nonzero determinant μ satisfy the seven signed relations in rows 1–7 of (2), with $M_{10} = M_2$ and $M_5 = M_{13}$. Their root and covector spans cannot both have dimension three.*

Proof. Reorder the crossings so that the propagation comes first:

$$(9,14,15,+),\ (15,9,2,+),\ (8,2,3,-),\ (14,3,4,+),\ (3,14,13,-),$$
$$(4,9,8,+), \qquad (2,13,4,+).$$

Here the rows with over-arcs $3, 4, 2$ and output arcs $13, 8, 4$, respectively, solve the corresponding prefix relations for the other under-arc. The first five crossings propagate all the matrices from M_8, M_{14}, M_9. If both spans have dimension three, the corresponding pairs $(u, f), (v, g_0), (w, j)$ are separately independent. Set

$$x = f(v), \quad X = g_0(u), \quad y = f(w), \quad Y = j(u), \quad z = g_0(w), \quad Z = j(v), \qquad \eta = 1 - \mu,$$
$$h = 1 + zZ/\mu, \qquad t = -zx/\mu + hy, \qquad \ell = ZX + hY,$$
$$\kappa = tX/\mu + z(h - \eta/\mu), \qquad \Lambda = -\ell x + (\eta + h)Z.$$

In the bases (u, v, w) and (f, g_0, j), propagation gives

i	u_i	f_i
2	$(0, -z/\mu, h)$	$(0, Z, h)$
3	$(t/\mu, -z/\mu, h)$	$(-\ell, Z, h)$
4	$(t/\mu, -z/\mu - \kappa, h)$	$(-\ell, Z + \Lambda/\mu, h)$
13	$(\Lambda t/\mu^2, 1 - \Lambda z/\mu^2, \Lambda h/\mu)$	$(\kappa\ell, 1 - \kappa Z, -\kappa h).$

For the first row, $M_{15} = M_9 M_{14} M_9^{-1}$ has pair $(v - Zw, g_0 + (z/\mu)j)$, and $M_2 = M_{15} M_9 M_{15}^{-1}$. The next two rows conjugate by M_8^{-1} and M_{14}, respectively, with $t = f(u_2)$, $\ell = f_2(u)$ and $\kappa = g_0(u_3)$, $\Lambda = f_3(v)$. The last row uses $M_{13} = M_3^{-1} M_{14} M_3$.

At the crossing $(4, 9, 8, +)$, put $P = f_4(w)$ and $Q = j(u_4)$. The first and third coefficients of $(M_4 w, j M_4^{-1}) = (\gamma u, \gamma^{-1} f)$ give

$$-Pt/\mu = \gamma, \qquad Ph = 1, \qquad -Q\ell/\mu = \gamma^{-1}, \qquad Qh/\mu = -1.$$

Thus P, Q, t, ℓ, h are nonzero. The middle coefficients give $\kappa = -z/\mu$ and $\Lambda = -\mu Z$. At $(2, 13, 4, +)$ the M_2 pair has zero first coefficients. Comparing the first coefficients of the pairs of M_{13} and $M_2^{-1} M_4 M_2$ therefore gives

$$\Lambda t/\mu^2 = \beta t/\mu, \qquad \kappa\ell = -\beta^{-1}\ell$$

with $\beta \neq 0$. Cancelling t, ℓ yields $zZ = \kappa\Lambda = -\mu$. This makes $h = 0$, contrary to $Ph = 1$. □

For an irreducible representation in Cornwell's correspondence, the root span is nonzero and invariant, hence equals V. The common kernel of the covectors is the fixed subspace and is zero, so the covectors span V^*. Lemma 2 bounds the dimension by $b - 1$ and proves the augmentation inequality in Theorem 1.

4 Hyperbolicity from two successive fillings

4.1 A circle around the moving strands

Set $\rho_b = \sigma_{b-1} \cdots \sigma_4$ and $\theta_d = \sigma_2 \cdots \sigma_{b-2}$. The braid relation gives $\rho_b \delta_b \rho_b^{-1} = \theta_d$. For instance, conjugation of σ_3 by σ_4^{-1} gives $\sigma_3 \sigma_4 \sigma_3^{-1}$ when $b = 5$. In the step from b to $b + 1$, the new letter σ_{b-1} of θ_{d+1} is conjugated by $\rho_b^{-1} \sigma_b^{-1}$, giving σ_b because $\sigma_b^{-1} \sigma_{b-1} \sigma_b = \sigma_{b-1} \sigma_b \sigma_{b-1}^{-1}$. The earlier letters are unchanged by σ_b before conjugating by ρ_b^{-1}. It follows that the two braid words

$$Q_b = \rho_b U \rho_b^{-1} \theta_d^{d+1}, \qquad Q_b' = \rho_b U \rho_b^{-1} \theta_d$$

are convenient starting points for a twist on the d consecutive strands in positions $2, \ldots, b - 1$.

Add strand $b + 1$ and append

$$P_b = \sigma_b \sigma_{b-1} \cdots \sigma_3 \sigma_2^2 \sigma_3 \cdots \sigma_{b-1} \sigma_b^{-1}.$$

The last strand closes to an unknot C, bounding a disk pierced once by each strand in positions $2, \ldots, b - 1$ and missing the other strands. One way to see the disk is to factor P_b as $A_{2,b+1} \cdots A_{b-1,b+1}$, where

$$A_{i,b+1} = \sigma_b \cdots \sigma_{i+1} \sigma_i^2 \sigma_{i+1}^{-1} \cdots \sigma_b^{-1}.$$

Each factor pushes the last puncture once around puncture i. The stems in this ordered product run along the same side of the adjacent punctures, so their concatenation bounds an oval around precisely those punctures. Equivalently, in the closure of the last strand, its two opposite crossings across strand b make a cancelling detour. The remaining oval passes over the selected strands on the outward trip and under them on the return. This gives the claimed disk in the slab of P_b, including the two outside positions. The knot component of $\widehat{Q_b P_b}$ has the permutation already computed in Section 2; the same is true for Q_b'.

For a disk-bounding circle with this marking, filling along $(1,-q)$ means killing $\mu_C - q\lambda_C$, where μ_C is a positive meridian and λ_C the preferred disk longitude. A disk twist on the solid torus obtained by removing C takes this slope to μ_C. Localizing the twist to the slab inserts q full twists on the disk-piercing strands. To check the sign, put $w = a_1 \cdots a_d$ for the selected meridians and c for the circle meridian. Tracing the outward and return crossings of the oval gives the selected outputs $c^{-1}a_i c$ and circle output $(wc)^{-1}c(wc)$. The return has crossed the whole ordered tuple, which contributes w. The two outside crossings conjugate the outside meridian by inverse powers of the initial and final circle labels and cancel after closure. The closure relation is $[c,w]=1$, and λ_C is represented by w, the boundary of the punctured disk. Filling gives $c = w^q$. By the Hurwitz formula, θ_d^d conjugates the whole selected tuple by w^{-1}, so the geometric disk twist inserts θ_d^{dq} in our convention.

Let $M_b = \mathrm{Ext}(\widehat{Q_b P_b})$ and $M_b' = \mathrm{Ext}(\widehat{Q_b' P_b})$, where $\mathrm{Ext}(L)$ denotes the link exterior. The preceding disk twist identifies M_b with M_b' as exteriors without a fixed peripheral basis, since their knot braids differ by one full twist on the disk. In the original marking of M_b we have

$$M_b\big(C : (1, -d(d+1)k)\big) \cong \mathrm{Ext}(K_{b,k}). \tag{3}$$

Indeed, the inserted power of θ_d is $d^2(d+1)k$. Conjugating the resulting braid by ρ_b^{-1} gives the word defining $K_{b,k}$.

4.2 A single exterior for the first filling

Consider the six-strand braid

$$R = \sigma_4\sigma_3\sigma_2^2\sigma_3\sigma_4\sigma_5^{-1}\sigma_4 U \sigma_4^{-1}\sigma_2\sigma_3\sigma_5$$

and the seven-strand suffix $D = \sigma_6\sigma_5\sigma_4^2\sigma_5\sigma_6^{-1}$. Set $N = \mathrm{Ext}(\widehat{RD})$. The closure of R has two components, a knot component containing U and a circle. The fourth and fifth closure arcs lie on these different components. These assignments also follow by tracing the strand permutation of R, which fixes position five and cycles the other five positions. The new last component D_0 bounds a disk around positions four and five, by the same oval construction as for P_b. Thus N has three boundary tori, and filling the new circle along the disk-marked slope gives

$$N\big(D_0 : (1,-q)\big) \cong \mathrm{Ext}(\widehat{R\sigma_4^{2q}}) \qquad (q \in \mathbb{Z}). \tag{4}$$

Lemma 4. *For every $b \geq 5$, the oriented link $\widehat{Q_b' P_b}$ is isotopic to $\widehat{R\sigma_4^{2(b-5)}}$, with the knot and circle components identified.*

Here is how the isotopy works. After braid conjugation and commutation,

$$\sigma_3^{-1}(U\delta_b)\sigma_3 = (\sigma_3^{-1}U\sigma_2\sigma_3)\sigma_4\sigma_5\cdots\sigma_{b-1}.$$

On the knot component alone this is an iterated positive stabilization. In the link, the disk of C meets the additional strands, so the corresponding curls cannot simply be removed. First cancel the detour of the circle and the two sides of the conjugating braid. The outer crossings then form a ladder along the circle. Slide each successive triangle through the already formed clasps by two Reidemeister III moves per clasp. At its end a Reidemeister III move exposes a curl, and a Reidemeister I move leaves one more two-crossing positive clasp. Repeating this leaves the $b=5$ diagram with $b-5$ clasps in the band of the fourth and fifth closure arcs of R.

Appendix A proves the isotopy by specifying the moves, the induction on the ladder, and the identification of that band.

By Lemma 4 and (4),

$$M_b \cong N\big(D_0 : (1, -(b-5))\big) \quad \text{as exteriors.}$$

This homeomorphism is used to transfer hyperbolicity. The second filling (3) uses the original disk marking of M_b. Twisting around either circle can change the expression of the other circle's longitude, so no common longitude basis is required for the two fillings.

4.3 Three finite hyperbolicity certificates

The computation certifies the complete hyperbolic structures of N, M_5, M_6, where M_5, M_6 use Q_b, with its full disk twist, in the literal braid $\widehat{Q_b P_b}$. Table 1 records the sizes of the input diagrams and certified triangulations. The two direct tests for M_5, M_6 give explicit bridge numbers covered by the theorem regardless of the threshold obtained from N.

Exterior	Diagram crossings	Cusps	Tetrahedra
N	32	3	35
M_5	32	2	31
M_6	43	2	34

Table 1: Literal braid diagrams and complete ideal triangulations for the three hyperbolicity certificates. Crossings are counted in the given projection.

Each exact input binds a planar-diagram code and its components to the braid, checking every crossing port and every closure identification. The exterior of that diagram is constructed in Spherogram 2.4.1 and SnapPy 3.3.2. Its decorated triangulation signature is checked against the retained one with the component marking, and the face pairings and gluing equations of the reloaded triangulation are checked. SnapPy under SageMath 10.9 then applies a Krawczyk interval test at 100 bits to both the fresh exterior and the retained triangulation. For the analytic criterion, a Krawczyk inclusion certifies a solution to a square subsystem of the shape equations in the interval box. The logarithmic edge and cusp equations are checked in the correct branches, and every shape has positive imaginary part. Together with the subsystem reduction, the positivity, gluing and completeness checks give a complete hyperbolic structure on the triangulated exterior [4, Sections 2–4]. Exact inputs, software pins, rational interval bounds and the replay procedure are supplied in the computational supplement. The proof uses these three finite certificates and the written diagram induction.

4.4 Proof of the prime-family conclusion

Since N is complete and finite-volume hyperbolic, Thurston's hyperbolic Dehn filling theorem [5, Theorem 5.8.2] applies to the D_0 cusp with the other two cusps unfilled. The slopes $(1, -(b-5))$ escape every finite set as b grows. Thus M_b is hyperbolic for every sufficiently large b, as well as for $b = 5, 6$ by the direct certificates. For any such b, apply the theorem to M_b on the C cusp. The slopes in (3) escape every finite set as k grows, so all sufficiently large $K_{b,k}$ are hyperbolic. A hyperbolic knot is prime. Indeed, a composite knot group is the amalgam of the nontrivial summand groups over their meridian, and the two summand longitudes lie

outside that amalgamating subgroup by peripheral injectivity. They commute with the common meridian and fail to commute with one another by amalgam normal form. The centralizer of a nonidentity element of a torsion-free discrete subgroup of $\mathrm{PSL}_2(\mathbb{C})$ is abelian, as is seen by putting the element in parabolic or loxodromic normal form.

For a fixed such b, the lengths ℓ_k of the second filling slopes on an embedded horotorus tend to infinity, since they are the norms of $\mu_C - d(d+1)k\lambda_C$ in a flat lattice with $\lambda_C \neq 0$. For sufficiently large k the fillings are hyperbolic and $\ell_k > 2\pi$. The volume inequality of Futer, Kalfagianni and Purcell [2, Theorem 1.1] and strict volume decrease under proper hyperbolic filling [5, Theorem 6.5.6] give

$$\left(1 - \left(\frac{2\pi}{\ell_k}\right)^2\right)^{3/2} \mathrm{vol}(M_b) \;\leq\; \mathrm{vol}\big(\mathrm{Ext}(K_{b,k})\big) \;<\; \mathrm{vol}(M_b).$$

The volumes converge to $\mathrm{vol}(M_b)$, and by Mostow–Prasad rigidity each hyperbolic exterior type has one volume. A finite set of exterior types would have a maximum volume strictly below $\mathrm{vol}(M_b)$. Thus there are infinitely many knot types for that b. Together with the algebraic bounds, this proves Theorem 1.

Computational supplement. The accompanying supplement supplies the exact planar diagrams, decorated triangulations, face pairings, gluing equations, rational interval enclosures, and replay scripts for the hyperbolicity certificates in Section 4.3. It also supplies the finite diagram moves and checks of the port conventions used in Appendix A. The algebraic and diagram inductions in the article establish the unrestricted parameter statements.

AI assistance and review. ChatGPT (OpenAI) assisted with mathematical arguments, literature checks, exposition, proof review and verification code.

A The oriented diagram isotopy

We prove Lemma 4 in the spherical braid projection. The proof fixes the crossings of U and keeps track of the two arcs where the new clasps are inserted.

A.1 Port convention and initial cancellations

A crossing has ports $0, 1, 2, 3$ in counterclockwise order. The even pair is the understrand and the odd pair the overstrand. A positive letter uses inputs $(0, 3)$ and outputs $(1, 2)$ in left-to-right order. A negative letter uses inputs $(1, 0)$ and outputs $(2, 3)$. On each strand, connect its last output to its first input to close the braid. Write $X.j$ for port j of crossing X and take port indices modulo four.

Put $r = b-4$ and number the crossings of $Q_b'P_b$ from zero. Cancel $3b+3$ with $5b$, followed by i with $2r + 13 - i$ for $0 \leq i < r$, in increasing order. The first pair consists of the two crossings in the circle detour. In each pair (X, Z) the bigon has edges $X.2$–$Z.0$ and $X.3$–$Z.3$. The signs are opposite, with one branch over at both crossings. These conditions specify Reidemeister II cancellations.

The indexing of the uncancelled crossings and the neighbours in the successive bigons can be obtained as follows. Name the 14 crossings of U by $F_j = r + j$. Use $Y_i = 2b + 6 + i$ for the $d-1$ crossings of θ_d, and set $u_j = 3b + 4 + j$, $v_j = 5b - 1 - j$ for $0 \leq j < d$, the crossings on the

descending and returning parts of P_b. The detour cancellation connects 0.3 to $(2b+5).3$ and $u_0.3$ to $v_0.2$. In the resulting first bigon and at each later step i, the four outside neighbours of $X = i,\ Z = 2b+5-i$ are

$$\begin{array}{l|l} X.0 & v_i.1 \\ X.1 & (i+1).3 \quad \text{if } i < r-1, \quad F_2.0 \quad \text{if } i = r-1 \\ Z.1 & (Z-1).3 \\ Z.2 & Y_{r-i}.3. \end{array}$$

The cancellation connects $v_i.1$ to $Y_{r-i}.3$ and wires the next bigon, with the last step joining $F_2.0$ to $F_{13}.3$. This describes the cancellations by induction. The listed neighbours are obtained from the port rule by following the consecutive crossings of $\rho_b^{-1}\theta_d$ and the return of P_b. In particular the pairs use no crossing from U.

Let $A = F_{12}.1,\ B = F_{13}.2,\ C = F_0.3,\ E = F_1.3$. The edges of the remaining diagram outside U are specified by their port neighbours in Table 2. The Y_i's follow the consecutive crossings of θ_d, with $Y_i.2$ proceeding to $Y_{i+1}.0$, or to $u_0.0$ at the end. The two circuits past the circle follow the u_j's in order and the v_j's in reverse order. At the doubled σ_2 the two crossings u_{d-1} and v_{d-1} meet directly. The r joins from the cancelled bigons give the attachments from v_i to Y_{r-i}. With the four unchanged attachments to U these traces give the table. All crossings in it are positive.

Crossing	Port 0	Port 1	Port 2	Port 3
Y_0	A	$u_{d-1}.0$	$Y_1.0$	B
$Y_i,\ 1 \le i \le d-2$	$Y_{i-1}.2$	$u_{d-1-i}.0$	$Y_{i+1}.0$ or $u_0.0$	$v_{d-2-i}.1$
u_0	$Y_{d-2}.2$	$u_1.3$	$v_0.3$	$v_0.2$
$u_j,\ 1 \le j \le d-2$	$Y_{d-1-j}.1$	$u_{j+1}.3$	$v_j.3$	$u_{j-1}.1$
u_{d-1}	$Y_0.1$	$v_{d-1}.0$	$v_{d-1}.3$	$u_{d-2}.1$
v_0	$v_1.2$	$Y_{d-2}.3$	$u_0.3$	$u_0.2$
$v_j,\ 1 \le j \le d-3$	$v_{j+1}.2$	$Y_{d-2-j}.3$	$v_{j-1}.0$	$u_j.2$
v_{d-2}	$v_{d-1}.2$	E	$v_{d-3}.0$	$u_{d-2}.2$
v_{d-1}	$u_{d-1}.1$	C	$v_{d-2}.0$	$u_{d-1}.2$

Table 2: Port neighbours after the initial cancellations. The Y_i port 2 neighbour is $u_0.0$ at $i = d-2$. Every edge is reciprocal, including the ones meeting U.

A.2 Two local moves and the induction

Write $(X,a),(Y,c),(Z,e)$ for the triangle with edges

$$X.(a+1)\text{–}Y.c, \qquad Y.(c+1)\text{–}Z.e, \qquad Z.(e+1)\text{–}X.a.$$

Consecutive ports make this a face in the oriented spherical rotation system. The projection is connected and these faces are empty disks. For the Reidemeister III moves below the edges have respectively two underports, two overports, and one of each. They are the bottom, top and middle branches required for the move.

First consider the triangle $(u,3),(t,2),(v,1)$ with an existing clasp attached, having edges $u.1$–$w.0$ and $u.2$–$w.3$. Use the six external endpoints in the first row of the table below, in the cyclic order $(e_0,e_1,e_4,e_5,e_3,e_2)$; the inputs are e_0,e_2,e_3. Apply Reidemeister III, first at this triangle and then at $(w,3),(v,2),(t,1)$. The clasp edges persist, and the other internal edges

become $w.1$–$t.0$, $w.2$–$v.0$, $t.3$–$v.1$. Tracing the three strands between the six endpoints gives the second row:

	e_0	e_1	e_2	e_3	e_4	e_5
before	$t.0$	$t.1$	$v.0$	$v.3$	$w.1$	$w.2$
after	$u.0$	$t.1$	$u.3$	$v.3$	$t.2$	$v.2.$

Thus the triangle can pass one clasp relative to all six external endpoints.

For the same triangle at the cap (Figure 1), use the extra edge $u.2$–$v.3$ and the first row below. The boundary order is (e_0, e_1, e_2, e_3), with inputs e_0, e_3. The first Reidemeister III move puts t on the edge from $u.2$ to $v.3$, with $u.2$–$t.0$, $t.1$–$v.3$ and a monogon $t.2$–$t.3$. Remove the monogon by Reidemeister I. The two crossings left form a positive clasp with edges $u.1$–$v.0$, $u.2$–$v.3$ and the external attachments in the second row:

	e_0	e_1	e_2	e_3
before	$t.0$	$t.1$	$u.1$	$v.0$
after	$u.0$	$v.1$	$v.2$	$u.3.$

In particular this is an ordinary positive full twist between the two incoming strands. Both local rewrites keep the cyclic boundary orders and orientations.

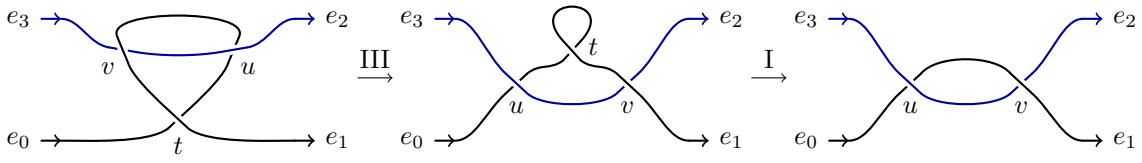


Figure 1: The signed cap move. The black strand runs from e_0 to e_1, and the blue strand from e_3 to e_2. Gaps mark the underpasses. All crossings are positive. The type III move on u, t, v exposes the curl at t, and the type I move removes it while fixing the four boundary endpoints.

Now put $q = d - 3$. At stage s, for $0 \le s < q$, set $t = Y_{d-2-s}$. There are already s clasp pairs (u_j, v_j) for $j < s$. Each has its two clasp edges, and

$$v_j.1\text{–}u_{j+1}.0, \qquad v_j.2\text{–}u_{j+1}.3.$$

The moving triangle begins at $(u_0, 3), (t, 2), (v_s, 1)$. At $s = 0$ the triangle and cap are in Table 2. At each u_j for $j < s$, use the first local rewrite with $w = v_j$, $v = v_s$. The two former attachments of w to u_{j+1} now attach $t.2$ and $v_s.2$ to u_{j+1}, giving the triangle at u_{j+1}. This leaves $u_s.2$–$v_s.3$ in place. At u_s, the cap rewrite removes t and gives the clasp (u_s, v_s).

To see the next stage, track the four ends of the unchanged part of the ladder. At the start of stage s, $t.0$ is attached to $Y_{d-3-s}.2$ and $v_s.0$ to $v_{s+1}.2$. The first rewrite sends those attachments to $u_0.0$ and $u_0.3$, whether it is at a clasp or at the cap. Later moves in the stage keep them there. The cap rewires $t.1$–$u_{s+1}.0$ and $u_s.1$–$u_{s+1}.3$ to the two new edges from $v_s.1, v_s.2$. The next triangle and cap therefore satisfy the same hypotheses. This proves the induction for every d.

At its end $Y_2, \dots, Y_{d-2}$ have been deleted. The diagram consists of the $d = 3$ ladder with indices Y_0, Y_1 and $u_q, u_{q+1}, u_{q+2}, v_q, v_{q+1}, v_{q+2}$, and q clasp pairs inserted between the two arcs $Y_1.2$–$u_q.0$ and $v_q.2$–$u_q.3$. The first endpoint of each arc now leads into the first clasp (or directly to u_q if $q = 0$). The two edges from v_j to u_{j+1} then lead to the next clasp or to the base ladder. All other edges of the base ladder remain as specified in the table, and the crossings of U are fixed.

A.3 Identifying the insertion band in R

Number the crossings of the literal word R from zero. Its fourth and fifth closure arcs run from 24.2 to 0.0 and from 25.1 to 0.3. Cut those two arcs just before crossing zero, leaving a named incoming and outgoing end for each arc. The Reidemeister II pairs $(6, 25)$ and $(7, 22)$ cancel with the four ends open. For the first pair the bigon edges are 6.0–25.2, 6.3–25.3. For the second they are 7.2–22.0, 7.3–22.3 after the first cancellation. The two incoming ends and the fourth outgoing end stay attached to their ports. The fifth outgoing end moves from 25.1 to 5.2. Neither cancellation meets the slab at the cut. The resulting 22-crossing projection, with the arcs reclosed, is the $d = 3$ ladder. The port bijection has no rotations and is given by

	F_j	Y_0	Y_1	u_0	u_1	u_2	v_0	v_1	v_2
crossing of R	$8+j$	23	24	0	1	2	5	4	3.

This is verified by the braid port rule, including the edges of U and the four attachments in Table 2. The cut arcs correspond precisely to $Y_1.2$–$u_0.0$ and $v_0.2$–$u_0.3$. The marked ends identify the actual fourth/fifth strand band before the first crossing of R, including both boundary orientations. In the closed braid a positive full twist in that band can be written at the end of R. Each clasp from the induction has the port pairing of σ_4^2 in this band, so the resulting projection is the twice-reduced diagram of $\widehat{R\sigma_4^{2q}}$. The oriented moves preserve the component containing U and the other component. Since $q = b - 5$, this proves Lemma 4.

References

[1] C. R. Cornwell, *KCH representations, augmentations, and A-polynomials*, J. Symplectic Geom. **15** (2017), 983–1017. doi:10.4310/JSG.2017.v15.n4.a2.

[2] D. Futer, E. Kalfagianni, and J. S. Purcell, *Dehn filling, volume, and the Jones polynomial*, J. Differential Geom. **78** (2008), 429–464. doi:10.4310/jdg/1207834551.

[3] H. Gao, S. Gu, Z. Li, and J. Wang, *Meridional ranks of iterated Whitehead doubles*, preprint, 2026. arXiv:2611.15673v1.

[4] N. Hoffman, K. Ichihara, M. Kashiwagi, H. Masai, S. Oishi, and A. Takayasu, *Verified computations for hyperbolic* 3*-manifolds*, Exp. Math. **25** (2016), 66–78. doi:10.1080/10586458.2015.1029599.

[5] W. P. Thurston, *The Geometry and Topology of Three-Manifolds*, Princeton lecture notes, electronic edition 1.1, 2002. Electronic edition.